
Gauge Equivariant Neural Networks for 2+1D U(1) Gauge Theory Simulations in Hamiltonian Formulation

Anonymous Author(s)

Affiliation

Address

email

Abstract

1 Gauge Theory plays a crucial role in many areas in science, including high energy
2 physics, condensed matter physics and quantum information science. In quantum
3 simulations of lattice gauge theory, an important step is to construct a wave function
4 that obeys gauge symmetry. In this paper, we have developed gauge equivariant neural
5 network wave function techniques for simulating continuous-variable quantum
6 lattice gauge theories in the Hamiltonian formulation. We have applied the gauge
7 equivariant neural network approach to find the ground state of 2 + 1-dimensional
8 lattice gauge theory with U(1) gauge group using variational Monte Carlo. We have
9 benchmarked our approach against the state-of-the-art complex Gaussian wave
10 functions, demonstrating improved performance in the strong coupling regime and
11 comparable results in the weak coupling regime.

12 1 Introduction

13 Parametrized gauge equivariant functions play an increasingly important role in deep learning and
14 the quantum simulation literature. The historical importance of gauge equivariance in physics
15 literature originates from the gauge principle, according to which the action functional dictating the
16 interactions of fundamental fields must be invariant under symmetry transformations that depend
17 upon $d + 1$ -dimensional space-time. It follows from the gauge principle that the form of the action
18 functional is fixed in terms of equivariant features of the field arguments, up to a low-dimensional
19 undetermined parametrization called coupling parameters. Remarkably, the gauge principle is
20 sufficient to essentially completely determine the form of the quantum Hamiltonian H , leaving the
21 determination of its eigenmodes as a problem of gauge invariant function approximation. This paper
22 offers a new approach to the ground eigenvalue problem for a prototypical gauge theory in 2 + 1
23 dimensions known as the Kogut-Susskind model, by drawing on techniques from gauge equivariant
24 machine learning. In contrast to an existing literature which pursues Lagrangian formulation [25],
25 this paper works in the so-called Hamiltonian lattice gauge approximation, in which the spatial
26 manifold is approximated by a d -dimensional regular periodic grid graph (V, E) with vertices V
27 and edges E , and the space of fields is approximated by a high-dimensional manifold $\Omega = \prod_{e \in E} G$
28 given by the product of some compact Lie group G over the edges of the graph. The quantum
29 Hamiltonian H is approximated by a Schrödinger operator acting on the space of wave functions
30 $L^2(\Omega) = \bigotimes_{e \in E} L^2(G)$. A gauge transformation is represented by an element $g \in \Omega$ of the
31 configuration space, which acts locally on a given field configuration $x \in \Omega$ by conjugation, producing
32 a transformed field configuration, which we denote by $g \cdot x \in \Omega$. The gauge group correspondingly

33 acts wavefunctions $\psi \in L^2(\Omega)$ as $g \cdot \psi(x) = \psi(g^{-1} \cdot x)$ and the quantum Hamiltonian is equivariant
 34 with respect to the gauge group in the sense that $g \cdot (H\psi) = H(g \cdot \psi)$ for all $g \in \Omega, \psi \in L^2(\Omega)$.
 35 For the ground states of pure gauge theories with no matter, the wave functions satisfy the strict
 36 invariance property $g \cdot \psi = \psi$.

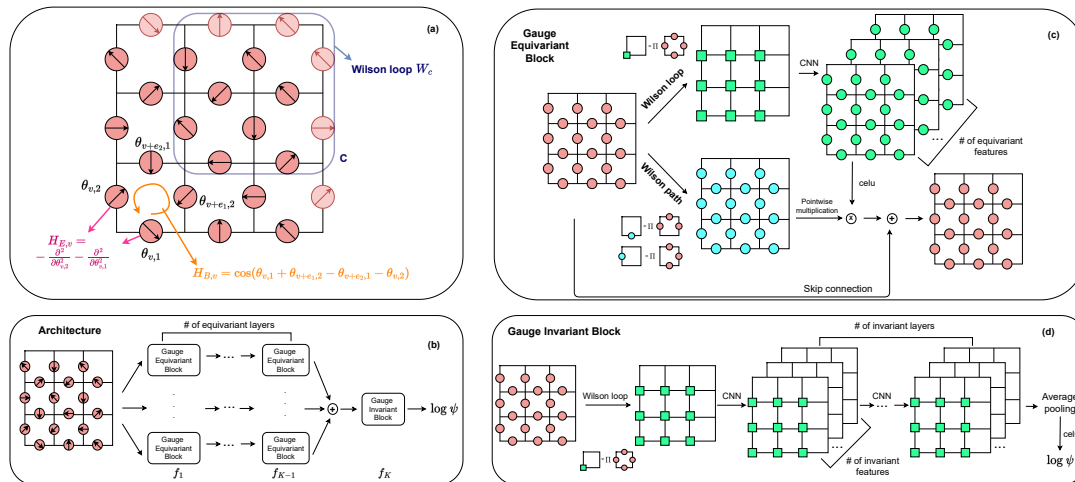


Figure 1: (a) Hamiltonian of U(1) lattice gauge theory. The gauge field is defined on each edge by a set of angular variables θ between $[0, 2\pi)$ and represented as $e^{i\theta}$. The Hamiltonian is defined in Eq. 3, where $H_{E,v}$ describes the kinetic energy of the gauge field for the vertex v and $H_{B,v}$ describes the magnetic energy. The faded arrows on edges are used to represent periodic boundary condition. (b) Gauge equivariant neural network architecture. (c) Gauge equivariant block. (d) Gauge invariant block.

37 With the advancement of machine learning, neural networks have been proposed [9] to represent
 38 quantum wave functions, which is known as neural network quantum states (NNQS). The key idea is
 39 to find a compact neural network representation of the high dimensional quantum state. It has been
 40 shown recently NNQS is able to approximate a large family of quantum state efficiently [41] and
 41 any quantum state supervised learning is also guaranteed to converge in the infinite width limit [34].
 42 In addition, NNQS also provides exact representations for many quantum states [17, 28, 27, 32, 30,
 43 15, 24, 46]. Recent research has applied NNQS to a variety of fields including condensed matter
 44 physics [20, 38, 11, 23, 33, 22, 47, 18, 42, 37, 5], high energy physics [30, 32, 3], and quantum
 45 information science [35, 10, 44]. It has been shown that NNQS can achieve state-of-the-art results
 46 for computing ground states and the real time dynamics properties of closed and open quantum
 47 systems [19, 40, 45, 49, 21, 36, 32, 31].

48 In this work, we develop the gauge equivariant neural network for U(1) lattice gauge theory. We
 49 focus on the U(1) Kogut-Susskind model, which is characterized by the simplest abelian Lie group
 50 $G = S^1$ and a $d = 2$ dimensional grid graph. We start by embedding $\Omega = \prod_{e \in E} S^1$ in a linear
 51 space \mathbb{C}^{N_1} on which the group action is defined, and introduce a sequence of hidden vector spaces
 52 $\mathbb{C}^{N_2}, \dots, \mathbb{C}^{N_K}, \mathbb{C}^{N_{K+1}}$ (with $N_{K+1} = 1$) and associated nonlinear mappings $f_k : \mathbb{C}^{N_k} \rightarrow \mathbb{C}^{N_{k+1}}$
 53 such that for all $g \in \Omega$ we have $f_k(g \cdot x) = g \cdot f_k(x)$ for $k \in \{1, \dots, K-1\}$ and $f_K(g \cdot x) = f_K(x)$
 54 for all relevant configurations x . The proposed trial wave function is given by

$$\psi = f_K \circ \dots \circ f_1 \quad (1)$$

55 In early work on Hamiltonian lattice gauge theories, non-compositional trial wave functions have
 56 been proposed in which $f_1 = \dots = f_{K-1} = \text{id}$ as the identity function. Here we have generalized
 57 the theory in [29] to the U(1) group and constructed continuous-variable gauge equivariant neural
 58 network for each f_k with much more powerful representation.

59 1.1 Related Work

60 In the machine learning community, group equivariant neural network for global symmetries have been
 61 considered in [13, 4, 26, 48, 43] and gauge equivariant neural networks have been recently introduced
 62 in [12, 14]. The authors in [12] used parallel transport techniques to construct convolutional neural
 63 networks defined on manifolds. In the physics community, gauge equivariant neural networks have
 64 been utilized to accelerate sampling and observables fitting in Lagrangian formulation of lattice
 65 field theories [25, 2, 1, 8, 16]. Gauge equivariant and gauge invariant neural networks [32, 30] have
 66 subsequently been used as trial wave functions for Hamiltonian formulation of lattice gauge theories
 67 with discrete gauge group including \mathbb{Z}_N theory and non-abelian Kitaev $D(G)$ model. In this work,
 68 we advance the state-of-art in [30] by constructing gauge equivariant neural network wave functions
 69 for continuous-variable lattice gauge theory and focus on the simplest abelian Lie group $U(1)$.

70 2 Background

71 We consider the 2+1D compact $U(1)$ pure gauge theory which is defined on a $L \times L$ square lattice
 72 with periodic boundary conditions. There are $V = L^2$ vertices and $2L^2$ edges, where the gauge
 73 field is a set of angular variables between $[0, 2\pi)$ on each edge. The space of field configurations is
 74 then given by $\Omega = [0, 2\pi)^{2L^2}$ and we represent a field configuration x by a 2-channel image x_δ with
 75 $\delta = 1, 2$, which represent the x-axis and the y-axis directions for the gauge field respectively.

$$x_\delta \equiv \begin{bmatrix} e^{i\theta_{(1,1),\delta}} & \dots & e^{i\theta_{(L,1),\delta}} \\ \vdots & & \vdots \\ e^{i\theta_{(1,L),\delta}} & \dots & e^{i\theta_{(L,L),\delta}} \end{bmatrix}, \quad \delta = 1, 2 \quad (2)$$

76 The Kogut Susskind Hamiltonian is defined as

$$H = \sum_{v \in V} \left[-\frac{g^2}{2} \left(\frac{\partial^2}{\partial \theta_{v,1}^2} + \frac{\partial^2}{\partial \theta_{v,2}^2} \right) - \frac{2}{g^2} \cos(\theta_{v,1} + \theta_{v+e_1,2} - \theta_{v+e_2,1} - \theta_{v,2}) \right] \quad (3)$$

77 where the first term describes the kinetic energy of the gauge field, the second term describes the
 78 magnetic energy (Fig. 1(a)) and g is the coupling constant.

79 The theory requires an additional satisfaction of gauge symmetry, such that the wave function is
 80 invariant under the following transformation on each vertex $v \in V$,

$$\theta_{v,\delta} \longrightarrow \theta_{v,\delta} + \alpha_{v+e_\delta} - \alpha_v, \quad \delta = 1, 2, \quad \alpha_v \in \mathbb{R} \quad (4)$$

81 For each gauge equivariant layer f_k where $l \in \{1, \dots, K-1\}$, it has been shown in [30] that the
 82 construction in Fig. 1(c) satisfies $f_k(g \cdot x) = g \cdot f_k(x)$ for any $g \in \Omega = \prod_{e \in E} \mathbb{Z}^N$. The property
 83 generalizes to the $U(1)$ group by taking $N \rightarrow \infty$. For the gauge invariant layer f_k , since it operates
 84 Wilson loop values which are gauge invariant objects, the construction in Fig. 1(d) is invariant
 85 under the transformation in Eq. 4 and satisfies $f_K(g \cdot x) = f_K(x)$ for $g \in \Omega = \prod_{e \in E} \mathbb{S}^1$. Hence,
 86 $\psi = f_K \circ \dots \circ f_1$ is invariant with respect to the transformation in Eq. 4 and respects the $U(1)$ gauge
 87 symmetry.

88 We search for the ground state through the variational principle

$$\min_w E = \frac{\langle \psi_w | H \psi_w \rangle}{\langle \psi_w | \psi_w \rangle} = \frac{\int_\Omega \psi_w^*(x) H \psi_w(x) dx}{\int_\Omega \psi_w^*(x) \psi_w(x) dx} \quad (5)$$

89 where w are the parameters of the gauge equivariant neural network. $\langle \cdot | \cdot \rangle$ denotes the L^2 inner
 90 product for $L^2(\Omega) = L^2([0, 2\pi)^{2L^2})$. The optimization is performed through variational Monte
 91 Carlo, where the gradients can be computed as follows:

$$\frac{\partial}{\partial w} E \approx \frac{2}{N} \sum_{x \sim |\psi_w|^2} \Re \left\{ E'_{\text{loc}}(x) \frac{\partial}{\partial w} \log \psi_w^*(x) \right\}. \quad (6)$$

92 where

$$E'_{\text{loc}}(x) = \frac{H\psi_w(x)}{\psi_w(x)} - \frac{1}{N} \sum_{x \sim |\psi_w|^2} \frac{H\psi_w(x)}{\psi_w(x)}. \quad (7)$$

93 The sampling $x \sim |\psi_w|^2$ is performed through Markov Chain Monte Carlo. Optimization is
 94 performed using the Stochastic Reconfiguration method[6].

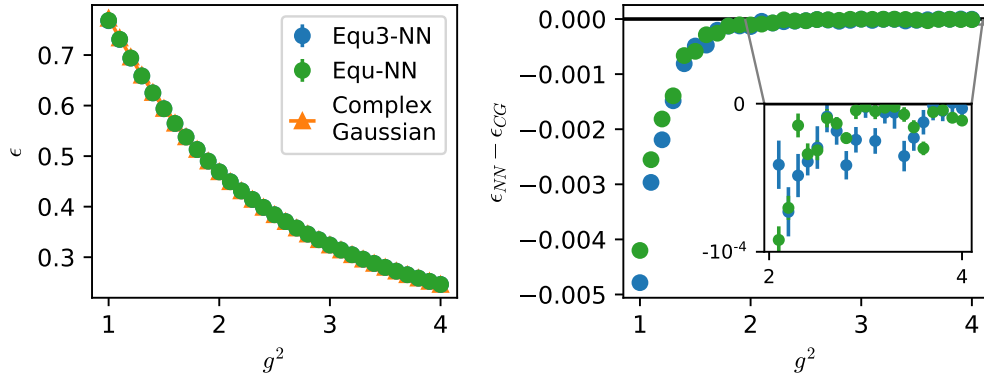


Figure 2: Left: Ground state energies of our variational ansatz compared with the data from [7] for $1 \leq g^2 \leq 4$ at $L = 8$. Right: Difference in ground state energies from our variational ansatz (ϵ_{NN}) and the complex Gaussian wave functions (ϵ_{CG}) from Ref.[7]. Inset shows energy differences in log-scale.

95 3 Model Architectures

96 We have developed a gauge equivariant neural network architecture as Fig. 1 shows. The general
 97 architecture of the gauge equivariant neural network is composed of gauge equivariant layers followed
 98 by gauge invariant layer which outputs the logarithmic of the wave function amplitude. The activation
 99 function in both equivariant and invariant blocks is $\text{celu}(z) = \text{elu}(\text{Re}(z)) + i * \text{elu}(\text{Im}(z))$ where
 100 z is a complex variable, $\text{elu}(x) = x$ for $x > 0$ and $\text{elu}(x) = \exp(x) - 1$ for $x \leq 0$. The network
 101 architecture is specified through the number of equivariant blocks, equivariant layers, equivariant
 102 features, invariant layers and invariant features. There are two gauge equivariant neural networks that
 103 we use in this work: Equ-NN and Equ3-NN. Equ-NN has only one gauge equivariant block in each
 104 equivariant layer, while Equ3-NN has three equivariant blocks in each layer. For all our simulations,
 105 we use 2 equivariant layers, 2 invariant layers, and 2 equivariant features for both Equ-NN and
 106 Equ3-NN. The number of invariant features depends on g^2 with four features being the default except
 107 for $g^2 = 0.5$ and 0.6 on the Equ-NN where we use three features.

108 4 Experiments

109 We compare our approaches with the state-of-the-art complex Gaussian method for both the strong
 110 coupling regime and the weak coupling regime. For the strong coupling regime, g is large and the
 111 kinetic energy term is more dominant such that a moderate system size L is sufficient for simulations.
 112 We consider g from 1 to 4 with increment 0.1 on $L = 8$ systems for experiments. Fig. 2(a) shows
 113 that both Equ-NN and Equ3-NN produce consistent energy decay as g increases. Fig. 2(b) shows the
 114 energy difference between the gauge equivariant neural networks and the state-of-the-arts complex
 115 Gaussian wave function method [7]. According to the variational principle, the lower energy indicates
 116 better performance. It can be seen that Equ-NN and Equ3-NN are both better than the complex
 117 Gaussian wave function and the energy performance gets better as g is closer to 1.

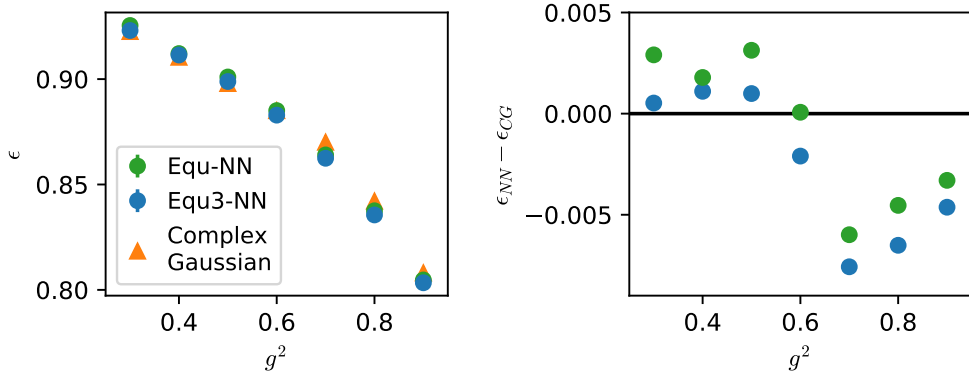


Figure 3: Ground state energy for $0.3 \leq g^2 \leq 0.9$ at $L = 14$ measured by gauge equivariant neural networks compared to the complex Gaussian wave functions from Ref.[7].

118 For the weak coupling regime, g is small so that the magnetic energy term in the Hamiltonian of Eq. 3
 119 plays a more important role and it requires larger system size to capture the physics. We consider
 120 experiments over g from 0.3 to 0.9 with increment 0.1 on $L = 14$ systems. Fig. 3 shows that the
 121 gauge equivariant neural network achieves better energy than the complex Gaussian wave function
 122 when $g \geq 0.6$ and comparable results when g is smaller. It is worth notice that in the $g \rightarrow 0$ limit, the
 123 ground state wave function becomes the trivial delta function in terms of the plaquette variable basis.
 124 However, this causes more challenging optimization for the gauge equivariant neural network. It may
 125 lead to the difference of the performance compared to the complex Gaussian wave function since a
 126 Gaussian is easier to approach a delta function.

127 To reflect the physics of the theory, one can consider the Wilson loop observable computed by

$$W_C = \frac{\langle \psi | \cos(\sum_{v \in C} \theta_{v,1} + \theta_{v+e_1,2} - \theta_{v+e_2,1} - \theta_{v,2}) | \psi \rangle}{\langle \psi | \psi \rangle} \quad (8)$$

128 where C is any contour on the lattice as Fig. 1(a) shows. Since the 2+1D pure U(1) gauge theory is
 129 confined for any g [39], the Wilson loop should decay exponentially as Eq. 9 with respect to the area
 130 included by the contour C .

$$W_C = e^{-\sigma R_1 \times R_2 - 2a(R_1 + R_2) + c} \quad (9)$$

131 where C is chosen to be a $R_1 \times R_2$ rectangle on the lattice. The exponential decay behaviours of the
 132 Wilson loops over $g^2 = 0.5, 0.6, 0.7$ of Equ-NN and Equ3-NN are shown in Fig. S1 and Fig. S2 in
 133 the Supplementary Materials.

134 5 Conclusion and Discussion

135 Gauge theories appear in a variety of contexts in physics, including high energy physics, condensed
 136 matter physics and quantum information science, and provides fundamental understandings of our
 137 universe. In this work, we have developed gauge equivariant neural networks for continuous-variable
 138 quantum lattice gauge theory with U(1) gauge group. We have applied the approach to find the
 139 ground state of 2+1D U(1) pure gauge theory and demonstrated better performance in the strong
 140 coupling regime and comparable results in the weak coupling regime over the state-of-the-arts
 141 complex Gaussian wave function. This is an important step that goes beyond the discrete lattice gauge
 142 theory [30] and opens up the possibilities of simulating the ground state and real time dynamics of
 143 lattice gauge theories with different symmetry groups. Future research will generalize the approach
 144 to non-abelian lattice gauge theories and study important physics such as confinement.

References

- [1] R. Abbott, M. S. Albergo, A. Botev, D. Boyda, K. Cranmer, D. C. Hackett, G. Kanwar, A. G. D. G. Matthews, S. Racanière, A. Razavi, D. J. Rezende, F. Romero-López, P. E. Shanahan, and J. M. Urban. Sampling qcd field configurations with gauge-equivariant flow models, 2022.
- [2] R. Abbott, M. S. Albergo, D. Boyda, K. Cranmer, D. C. Hackett, G. Kanwar, S. Racanière, D. J. Rezende, F. Romero-López, P. E. Shanahan, B. Tian, and J. M. Urban. Gauge-equivariant flow models for sampling in lattice field theories with pseudofermions, 2022.
- [3] C. Adams, G. Carleo, A. Lovato, and N. Rocco. Variational monte carlo calculations of a4 nuclei with an artificial neural-network correlator ansatz. *Physical Review Letters*, 127(2), Jul 2021.
- [4] B. Anderson, T.-S. Hy, and R. Kondor. Cormorant: Covariant molecular neural networks, 2019.
- [5] N. Astrakhantsev, T. Westerhout, A. Tiwari, K. Choo, A. Chen, M. H. Fischer, G. Carleo, and T. Neupert. Broken-symmetry ground states of the heisenberg model on the pyrochlore lattice. *Physical Review X*, 11(4), Oct 2021.
- [6] F. Becca and S. Sorella. *Quantum Monte Carlo Approaches for Correlated Systems*. Cambridge University Press, 2017.
- [7] J. Bender, P. Emonts, E. Zohar, and J. I. Cirac. Real-time dynamics in $2 + 1d$ compact qed using complex periodic gaussian states. *Phys. Rev. Research*, 2:043145, Oct 2020.
- [8] D. Boyda, G. Kanwar, S. Racanière, D. J. Rezende, M. S. Albergo, K. Cranmer, D. C. Hackett, and P. E. Shanahan. Sampling using $SU(n)$ gauge equivariant flows. *Phys. Rev. D*, 103:074504, Apr 2021.
- [9] G. Carleo and M. Troyer. Solving the quantum many-body problem with artificial neural networks. *Science*, 355(6325):602–606, 2017.
- [10] J. Carrasquilla, D. Luo, F. Pérez, A. Milsted, B. K. Clark, M. Volkovs, and L. Aolita. Probabilistic simulation of quantum circuits with the transformer, 2019.
- [11] K. Choo, T. Neupert, and G. Carleo. Two-dimensional frustrated j1j2 model studied with neural network quantum states. *Physical Review B*, 100(12), Sep 2019.
- [12] T. Cohen, M. Weiler, B. Kicanaoglu, and M. Welling. Gauge equivariant convolutional networks and the icosahedral cnn. In *International conference on Machine learning*, pages 1321–1330. PMLR, 2019.
- [13] T. S. Cohen and M. Welling. Group equivariant convolutional networks. 2016.
- [14] P. de Haan, M. Weiler, T. Cohen, and M. Welling. Gauge equivariant mesh cnns: Anisotropic convolutions on geometric graphs, 2020.
- [15] D.-L. Deng, X. Li, and S. Das Sarma. Quantum entanglement in neural network states. *Physical Review X*, 7(2), May 2017.
- [16] M. Favoni, A. Ipp, D. I. Müller, and D. Schuh. Lattice gauge equivariant convolutional neural networks. *Physical Review Letters*, 128(3), jan 2022.
- [17] X. Gao and L.-M. Duan. Efficient representation of quantum many-body states with deep neural networks. *Nature Communications*, 8(1):662, Sep 2017.
- [18] I. Glasser, N. Pancotti, M. August, I. D. Rodriguez, and J. I. Cirac. Neural-network quantum states, string-bond states, and chiral topological states. *Physical Review X*, 8(1), Jan 2018.
- [19] I. L. Gutiérrez and C. B. Mendl. Real time evolution with neural-network quantum states, 2020.

- 187 [20] X. Han and S. A. Hartnoll. Deep quantum geometry of matrices. Physical Review X, 10(1),
188 Mar 2020.
- 189 [21] M. J. Hartmann and G. Carleo. Neural-network approach to dissipative quantum many-body
190 dynamics. Phys. Rev. Lett., 122:250502, Jun 2019.
- 191 [22] J. Hermann, Z. Schätzle, and F. Noé. Deep neural network solution of the electronic schrödinger
192 equation, 2019.
- 193 [23] M. Hibat-Allah, M. Ganahl, L. E. Hayward, R. G. Melko, and J. Carrasquilla. Recurrent neural
194 network wave functions. Phys. Rev. Research, 2:023358, Jun 2020.
- 195 [24] Y. Huang and J. E. Moore. Neural network representation of tensor network and chiral states.
196 Phys. Rev. Lett., 127:170601, Oct 2021.
- 197 [25] G. Kanwar, M. S. Albergo, D. Boyda, K. Cranmer, D. C. Hackett, S. Racaniere, D. J. Rezende,
198 and P. E. Shanahan. Equivariant flow-based sampling for lattice gauge theory. Physical Review
199 Letters, 125(12):121601, 2020.
- 200 [26] R. Kondor, Z. Lin, and S. Trivedi. Clebsch-gordan nets: a fully fourier space spherical
201 convolutional neural network, 2018.
- 202 [27] Y. Levine, O. Sharir, N. Cohen, and A. Shashua. Quantum entanglement in deep learning
203 architectures. Physical Review Letters, 122(6), Feb 2019.
- 204 [28] S. Lu, X. Gao, and L.-M. Duan. Efficient representation of topologically ordered states with
205 restricted boltzmann machines. Phys. Rev. B, 99:155136, Apr 2019.
- 206 [29] D. Luo, G. Carleo, B. K. Clark, and J. Stokes. Gauge equivariant neural networks for quantum
207 lattice gauge theories, 2020.
- 208 [30] D. Luo, G. Carleo, B. K. Clark, and J. Stokes. Gauge equivariant neural networks for quantum
209 lattice gauge theories. Physical review letters, 127(27):276402, 2021.
- 210 [31] D. Luo, Z. Chen, J. Carrasquilla, and B. K. Clark. Autoregressive neural network for simulating
211 open quantum systems via a probabilistic formulation. Phys. Rev. Lett., 128:090501, Feb 2022.
- 212 [32] D. Luo, Z. Chen, K. Hu, Z. Zhao, V. M. Hur, and B. K. Clark. Gauge invariant autoregressive
213 neural networks for quantum lattice models, 2021.
- 214 [33] D. Luo and B. K. Clark. Backflow transformations via neural networks for quantum many-body
215 wave functions. Physical Review Letters, 122(22), Jun 2019.
- 216 [34] D. Luo and J. Halverson. Infinite neural network quantum states, 2021.
- 217 [35] M. Medvidović and G. Carleo. Classical variational simulation of the quantum approximate
218 optimization algorithm. npj Quantum Information, 7(1), Jun 2021.
- 219 [36] A. Nagy and V. Savona. Variational quantum monte carlo method with a neural-network ansatz
220 for open quantum systems. Phys. Rev. Lett., 122:250501, Jun 2019.
- 221 [37] Y. Nomura, A. S. Darmawan, Y. Yamaji, and M. Imada. Restricted boltzmann machine learning
222 for solving strongly correlated quantum systems. Physical Review B, 96(20), Nov 2017.
- 223 [38] D. Pfau, J. S. Spencer, A. G. D. G. Matthews, and W. M. C. Foulkes. Ab initio solution of the
224 many-electron schrödinger equation with deep neural networks. Phys. Rev. Research, 2:033429,
225 Sep 2020.
- 226 [39] A. M. Polyakov. Compact gauge fields and the infrared catastrophe. Physics Letters B, 59(1):82–
227 84, 1975.

- 228 [40] M. Schmitt and M. Heyl. Quantum many-body dynamics in two dimensions with artificial
229 neural networks. Physical Review Letters, 125(10), Sep 2020.
- 230 [41] O. Sharir, A. Shashua, and G. Carleo. Neural tensor contractions and the expressive power of
231 deep neural quantum states, 2021.
- 232 [42] J. Stokes, J. R. Moreno, E. A. Pnevmatikakis, and G. Carleo. Phases of two-dimensional spinless
233 lattice fermions with first-quantized deep neural-network quantum states. Physical Review B,
234 102(20), Nov 2020.
- 235 [43] N. Thomas, T. Smidt, S. Kearnes, L. Yang, L. Li, K. Kohlhoff, and P. Riley. Tensor field
236 networks: Rotation- and translation-equivariant neural networks for 3d point clouds, 2018.
- 237 [44] G. Torlai, G. Mazzola, J. Carrasquilla, M. Troyer, R. Melko, and G. Carleo. Neural-network
238 quantum state tomography. Nature Physics, 14(5):447–450, May 2018.
- 239 [45] F. Vicentini, A. Biella, N. Regnault, and C. Ciuti. Variational neural-network ansatz for steady
240 states in open quantum systems. Physical Review Letters, 122(25), Jun 2019.
- 241 [46] T. Viejra, C. Casert, J. Nys, W. De Neve, J. Haegeman, J. Ryckebusch, and F. Verstraete.
242 Restricted boltzmann machines for quantum states with non-abelian or anyonic symmetries.
243 Physical Review Letters, 124(9), Mar 2020.
- 244 [47] J. Wang, Z. Chen, D. Luo, Z. Zhao, V. M. Hur, and B. K. Clark. Spacetime neural network for
245 high dimensional quantum dynamics, 2021.
- 246 [48] M. Weiler, M. Geiger, M. Welling, W. Boomsma, and T. Cohen. 3d steerable cnns: Learning
247 rotationally equivariant features in volumetric data, 2018.
- 248 [49] N. Yoshioka and R. Hamazaki. Constructing neural stationary states for open quantum many-
249 body systems. Phys. Rev. B, 99:214306, Jun 2019.

250 **A Supplemental Material**

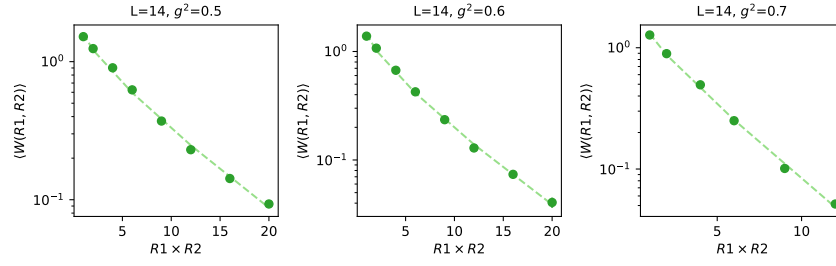


Figure S1: Wilson loops $\langle W(R_1, R_2) \rangle$ in the ground state in the small coupling regime, computed on a 14×14 lattice by model Equ-NN, as a function of the area $R_1 \times R_2$. The dash line fittings show the exponential decay of Wilson loops according to Eq. 9.

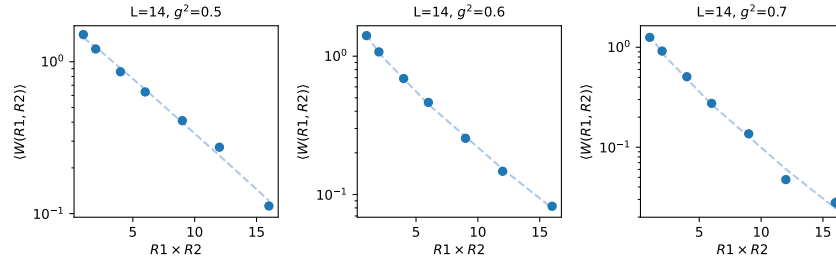


Figure S2: Wilson loops $\langle W(R_1, R_2) \rangle$ in the ground state in the small coupling regime, computed on a 14×14 lattice by model Equ3-NN, as a function of the area $R_1 \times R_2$. The dash line fittings show the exponential decay of Wilson loops according to Eq. 9.